

Scanning tunneling microscopy study of the ambient oxidation of passivated GaAs(100) surfaces

P. Moriarty, B. Murphy, and G. Hughes

Citation: *J. Vac. Sci. Technol. A* **11**, 1099 (1993); doi: 10.1116/1.578448

View online: <http://dx.doi.org/10.1116/1.578448>

View Table of Contents: <http://avspublications.org/resource/1/JVTAD6/v11/i4>

Published by the AVS: Science & Technology of Materials, Interfaces, and Processing

Related Articles

Novel techniques for modifying microtube surfaces with various periodic structures ranging from nano to microscale

J. Vac. Sci. Technol. B **31**, 011806 (2013)

Decomposition and phase transformation in TiCrAlN thin coatings

J. Vac. Sci. Technol. A **30**, 061506 (2012)

Surface modification of gold-carbon nanotube nanohybrids under the influence of near-infrared laser exposure

J. Vac. Sci. Technol. B **30**, 03D119 (2012)

Quantification of cesium surface contamination on silicon resulting from SIMS analysis

J. Vac. Sci. Technol. B **30**, 031203 (2012)

Surface functionalization of graphenelike materials by carbon monoxide atmospheric plasma treatment for improved wetting without structural degradation

J. Vac. Sci. Technol. B **30**, 03D107 (2012)

Additional information on *J. Vac. Sci. Technol. A*

Journal Homepage: <http://avspublications.org/jvsta>

Journal Information: http://avspublications.org/jvsta/about/about_the_journal

Top downloads: http://avspublications.org/jvsta/top_20_most_downloaded

Information for Authors: http://avspublications.org/jvsta/authors/information_for_contributors

ADVERTISEMENT

Instruments for advanced science

Gas Analysis



- dynamic measurement of reaction gas streams
- catalysis and thermal analysis
- molecular beam studies
- dissolved species probes
- fermentation, environmental and ecological studies

Surface Science



- UHV TPD
- SIMS
- end point detection in ion beam etch
- elemental imaging - surface mapping

Plasma Diagnostics



- plasma source characterization
- etch and deposition process reaction kinetic studies
- analysis of neutral and radical species

Vacuum Analysis



- partial pressure measurement and control of process gases
- reactive sputter process control
- vacuum diagnostics
- vacuum coating process monitoring

contact Hiden Analytical for further details

HIDEN
ANALYTICAL

info@hideninc.com
www.HidenAnalytical.com

CLICK to view our product catalogue 

Scanning tunneling microscopy study of the ambient oxidation of passivated GaAs(100) surfaces

P. Moriarty, B. Murphy, and G. Hughes

Department of Physics, Dublin City University, Glasnevin, Dublin 9, Ireland

(Received 9 November 1992; accepted 12 April 1993)

A scanning tunneling microscope (STM) operating in air has been used to study GaAs(100) surfaces which have been passivated in aqueous $P_2S_5/(NH_4)_2S$ and $P_2S_5/(NH_4)_2S_x$ solutions. The growth of native oxides under ambient conditions on these passivated surfaces has been monitored by STM. A spatial analysis of the oxide growth over $3 \times 3 \mu m^2$ areas indicates that the native oxide initiates as isolated islands across the surface which coalesce to form a uniform oxide layer. Evaluation of these surfaces in terms of peak-to-valley and root-mean-square roughness measurements indicates that surfaces treated in the $P_2S_5/(NH_4)_2S_x$ solution oxidize at a slower rate than those treated with the $P_2S_5/(NH_4)_2S$ solution. The repeated scanning of a particular area by the STM results in a significant increase in the local oxidation rate compared with surrounding areas which are scanned only once. The application of short high voltage pulses to the tip during an interruption in the scanning routine results in a greatly enhanced oxidation rate directly beneath the tip. Scanning tunneling spectroscopy characteristics, both I/V and $(dI/dV)/(I/V)$, reveal considerable differences in the band bending and consequently the density of surface states, present on the passivated and unpassivated surfaces.

I. INTRODUCTION

The modification of the electronic properties of GaAs surfaces due to treatment with aqueous ammonium sulfide solutions has recently been the subject of considerable investigation. These sulfur based treatments have been shown to reduce surface recombination velocity,^{1,2} increase photoluminescence (PL) intensity,³ and introduce a clear dependence of the Schottky barrier height on the work function of the contact metal.^{4,5} This latter effect indicates an unpinning of the Fermi level via a reduction in the high surface state density. A successful passivating layer must prevent surface oxidation. The presence of oxygen on the GaAs surface leads to the formation of both gallium and arsenic oxides. The enhanced thermodynamic stability of gallium oxides over arsenic oxides leads to the gradual reduction of arsenic oxides by neighboring gallium atoms resulting in the segregation of arsenic atoms.^{6,7} The segregation of the arsenic atoms following this reaction sequence is believed to cause the high density of surface states which pin the Fermi level.⁸ Photoemission studies by a number of groups have determined that the passivation of the GaAs surface by both $(NH_4)_2S$ and $(NH_4)_2S_x$ solutions is due to the presence of a sulfur overlayer, ~ 1 monolayer (ML) thick. While there is extensive evidence from these studies that sulfur bonds to both Ga and As surface atoms,⁹⁻¹³ others¹⁴ have reported evidence of only As-S bonding. Fan *et al.*¹⁵ have reported the increased passivating effects of $(NH_4)_2S_x$ solution when compared with a $(NH_4)_2S$ based solution due to the etching behavior of a reactive sulfur species only present in the former solution. Nannichi *et al.*¹⁶ have proposed that this is due to the more complete removal of the residual surface oxides by the $(NH_4)_2S_x$ etching solution. Oigawa *et al.*¹⁷ have estimated the etch rate of the $(NH_4)_2S_x$ solution to be $\sim 2-3$ nm/h at an etch temperature of $45^\circ C$.

A major problem affecting the long term stability of sulfur passivated GaAs surfaces as described above, is the inherent thermodynamic instability of gallium and arsenic sulfides with respect to the corresponding oxides.¹⁸ Lee *et al.*¹⁹ reported a fivefold increase in the PL intensity, when the GaAs surface was passivated using a $P_2S_5/(NH_4OH)$ solution, with the PL intensity remaining constant over ten days exposure to air. They suggested that the significant advantage offered by the addition of phosphorus compounds to the passivation treatment is the enhanced thermodynamic stability of phosphorus oxide over gallium oxide. This would mean that a surface phosphorus oxide could not be reduced by gallium, thereby inhibiting the reaction sequence which leads to arsenic segregation. Wang *et al.*²⁰ have used a wide range of techniques to characterise GaAs(100) surfaces passivated in $P_2S_5/(NH_4)_2S$ solutions both with and without additions of free sulfur. X-ray photoelectron spectroscopy (XPS) studies of the passivated surfaces revealed evidence of the presence of sulfur bound to both Ga and As surface atoms. An increase of PL intensity of up to 23 times the signal for the freshly etched surface was observed for surfaces passivated in $P_2S_5/(NH_4)_2S/S_x$. This treatment also yielded the surface with the slowest PL intensity degradation rate on exposure to air.

Richter and Hartnagel¹⁰ have used scanning tunneling microscopy (STM) to characterize the ambient oxidation of NH_4OH etched and $(NH_4)_2S$ passivated GaAs(100) surfaces. They reported a considerable increase in the electrical homogeneity of the sulphur passivated surface when compared with the NH_4OH etched surface. A comprehensive analysis of $P_2S_5/(NH_4)_2S$ treated GaAs(100) has recently been described by Dagata *et al.*²¹⁻²³ with the ultimate objective of preparing a surface which is topographically and chemically uniform. They pointed out that the STM image of a surface contains information on

both the surface topography and local electrical conductivity. This means that the presence of poorly conducting oxide regions on a "perfectly" flat surface would appear as variations in the surface topography due to the movement of the STM tip towards the surface in order to maintain a constant tunneling current. Therefore, variations in peak-to-valley (PV) and root-mean-square (RMS) roughness of these surfaces as a function of passivation procedure provide a very critical measurement of the surface topography and chemical uniformity.²² They have also reported an improved passivation due to the $P_2S_5/(NH_4)_2S$ treatment as compared with $(NH_4)_2S$ alone and have adapted the former treatment so as to make it compatible with STM imaging. Time-of-flight secondary ion mass spectroscopy (SIMS) and XPS studies carried out on these passivated surfaces suggested that the stability of the $P_2S_5/(NH_4)_2S$ passivated surface was as a result of the formation of an ordered ultrathin oxide and not due to sulfur termination.²²

In this study, the ambient oxidation of GaAs(100) surfaces passivated in both $P_2S_5/(NH_4)_2S$ and $P_2S_5/(NH_4)_2S_x$ solutions is investigated by STM over $3 \times 3 \mu m^2$ areas. Consistent differences were found in both initial PV and RMS roughness of these surfaces and significantly different rates of oxidation were observed. The chemical composition of the passivated surfaces was determined by Auger electron spectroscopy (AES) and the role of phosphorus in the passivation treatment was investigated. The effect of the scanning electric field of the STM on the oxidation process is discussed. STM tunneling spectroscopy characteristics for the passivated and unpassivated surfaces revealed significant differences in the density of surface states, manifested as a higher degree of band bending on the unpassivated (oxidized) surface. The Fermi-level position within the band gap region is also seen to move from near the conduction band edge, on well passivated samples, to approximately midgap for unpassivated samples and on regions of the passivated surface where a STM scan induced oxide has been formed.

II. EXPERIMENT

The samples used for STM investigation in this study were cut from commercially available *n*-type GaAs(100) wafers with a doping concentration of $2 \times 10^{18} \text{ cm}^{-3}$. Prior to passivation all samples were degreased and cleaned ultrasonically in de-ionized (DI) water, acetone, and methanol (HPLC grade). For $P_2S_5/(NH_4)_2S$ and $P_2S_5/(NH_4)_2S_x$ passivation, a procedure very similar to that described by Dagata *et al.*²² was followed. The sample was placed in concentrated H_2SO_4 for 1 min, etched in a room temperature $H_2SO_4:H_2O_2:H_2O$ (5:1:1) solution for 3 min with continual stirring and then plunged immediately into one of the two passivating solutions. An intermediate water rinse prior to placing the etched sample in the ammonium sulphide-based solutions was found by Dagata to significantly roughen the surface.²² The sulfur containing solutions were prepared by dissolving 1 g of P_2S_5 in 20 ml of either a $(NH_4)_2S$ or a $(NH_4)_2S_x$ solution and adding 60 ml of water. After leaving the sample in the solution for 10

min at room temperature, the passivating solution was heated to 50–60 °C for 10–15 min. Heating to higher temperatures or dissolving larger concentrations of P_2S_5 caused the solution to adopt a "milky" appearance, and the sample became caked in a thick sulfur layer. After removal from the passivating solution the sample was given a brief methanol (HPLC grade) rinse and carefully blown dry in nitrogen. The effect of a final DI water as opposed to a methanol rinse is discussed in the following section.

AES was performed with a retarding field analyzer which was also used for low-energy electron diffraction (LEED) studies of the passivated surfaces. All STM images were obtained at room temperature and under ambient pressure using the commercially available Nanoscope II from Digital Instruments, CA and platinum-iridium tips from the same supplier. Constant current mode (Nanoscope "Height" mode) was employed with a scan rate of 1.3 Hz, tunneling current of 1 nA, and a sample bias voltage of -3.8 V .

III. RESULTS AND DISCUSSION

A. Ambient STM imaging

Images of the chemically etched unpassivated surface, $P_2S_5/(NH_4)_2S$ and $P_2S_5/(NH_4)_2S_x$ treated surfaces after 15 min exposure to air are shown in Figs. 1(a)–1(c), respectively. The corresponding RMS roughness values (R_{app}), over representative $1 \mu m^2$ areas, are 8 nm for the unpassivated surface and 0.4 and 0.3 nm for the $P_2S_5/(NH_4)_2S$ and $P_2S_5/(NH_4)_2S_x$ treated surfaces, respectively. This method of using apparent roughness parameters to characterize the passivated surface has previously been employed by Dagata *et al.*,²² and the 0.4 nm R_{app} value noted for the surface treated in the $P_2S_5/(NH_4)_2S$ solution is in excellent agreement with the value determined by that group for a similar treatment. Slightly lower roughness parameters were consistently obtained on the $P_2S_5/(NH_4)_2S_x$ prepared surfaces. All the images displayed in Fig. 1 were captured after a single scan. AES spectra of both these passivated surfaces revealed the presence of sulfur and phosphorus. As was mentioned in Sec. I, the STM image is a convolution of the surface topography and the chemical homogeneity of the surface. The surface oxidation of GaAs leads to the physical disruption of the surface by the formation of stoichiometric oxides which in turn contribute to the chemical inhomogeneity which affects local conductivity. Therefore, we believe that it is reasonable to consider the apparent surface roughness as a relative measure of the extent of surface oxidation rather than simply reflecting the surface topography. Both of the passivating solutions used substantially reduce the topographical and chemical inhomogeneities apparent on the unpassivated surface.

As was mentioned in the Sec. II, the sulfur passivated surfaces had a final methanol rinse prior to being blown dry with nitrogen. Using DI water as opposed to methanol as the final rinse yielded surfaces comparable to Fig. 1(a). This behavior was also observed by Richter and Hartnagel,¹⁰ who found by XPS measurements, that a final

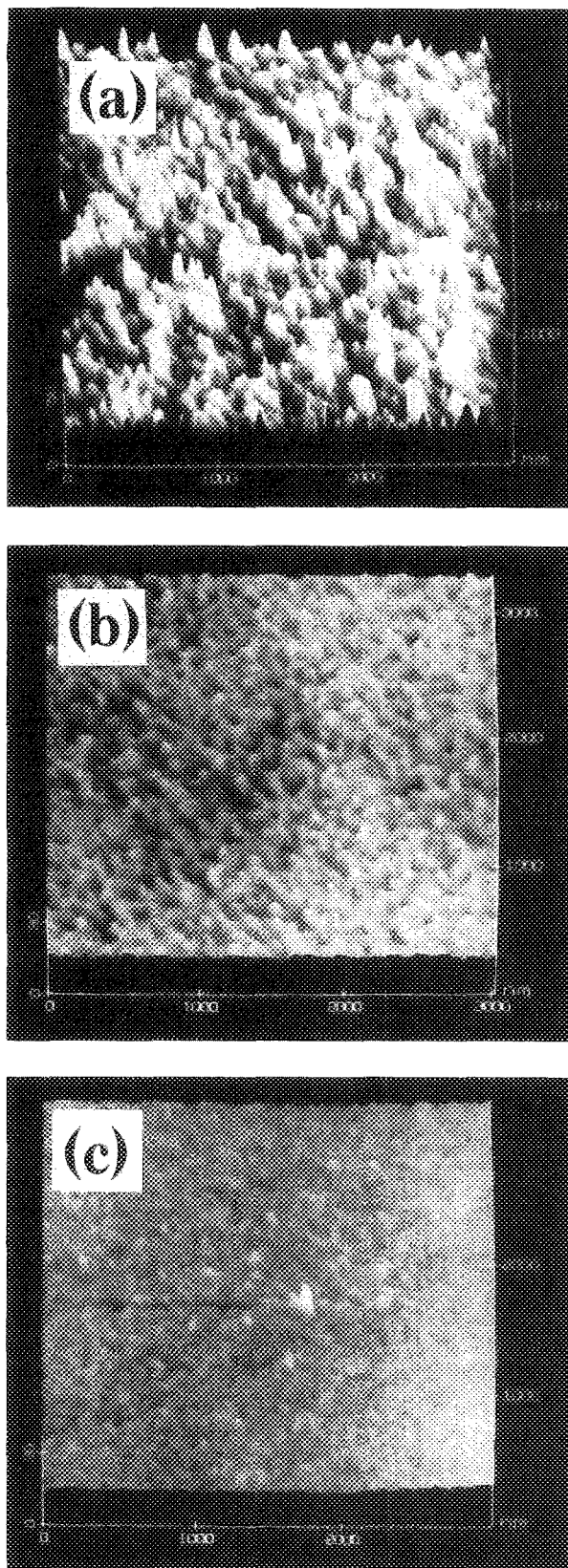


FIG. 1. STM images over $3 \times 3 \mu\text{m}^2$ areas, of the (a) chemically etched, (b) $\text{P}_2\text{S}_5/(\text{NH}_4)_2\text{S}$ treated, and (c) $\text{P}_2\text{S}_5/(\text{NH}_4)_2\text{S}/\text{S}_x$ treated GaAs(100) surface after 15 min exposure to air.

water rinse produced a surface much like the unpassivated surface with a large oxygen content in both the As and Ga $2p$ photoemission peaks. Wang *et al.*²⁰ also note that the PL intensity of the $\text{P}_2\text{S}_5/(\text{NH}_4)_2\text{S}/\text{S}_x$ treated surface, having undergone this final water rinse, decreased to that of the unpassivated surface. In order to determine whether the final water rinse altered the chemical composition of the passivated surfaces, we compared the AES spectra of surfaces rinsed in both DI water and methanol. These spectra revealed that a final water rinse removed phosphorus from the surface, while the methanol rinsed surface had phosphorus present. This removal of phosphorus by a final water rinse was also reported by Wang *et al.*²⁰ XPS studies, carried out by this group, on P_2S_5 treated surfaces indicated that the phosphorus was not bonded to the Ga or As surface atoms, but involved only in S-P and P-O bonding configurations. These observations would support the idea that the phosphorus is involved in the passivation mechanism by chemically reacting with adsorbed oxygen to form an oxide which is thermodynamically stable with respect to Ga or As oxides as previously proposed by Lee *et al.*¹⁹ Therefore, it would appear that the phosphorus plays a key role in stabilizing the passivated surface against oxidation.

One further sulfur treatment was applied to the GaAs(100) surface. After solvent cleaning and chemically etching as before, the sample was placed in a solution of $(\text{NH}_4)_2\text{S}_x$ overnight and then blown dry with nitrogen and placed in vacuum as described by Hirayama.²⁴ Auger spectra of this surface revealed a sulfur signal on this surface which was considerably larger than found for samples passivated in either of the P_2S_5 based treatments. Attempts to image this surface by STM after removal from vacuum were not successful due to excessively noisy and unstable tunneling images. We speculate that this is due to presence of loosely bound sulfur layers on the surface. These layers, under the influence of the scanning electric field are likely to cause STM image instability. We have found that by heating of the $(\text{NH}_4)_2\text{S}_x$ solution to 50°C and reducing the time that the sample is left in the solution to 10 min, that stable images on this sulfur passivated surface are possible, however, initial roughness values are substantially larger than those found on surfaces passivated in the P_2S_5 containing solutions. STM images taken of different areas across the passivated surfaces in this investigation revealed a large spread in the roughness values. Some isolated regions were found to have roughnesses as high as five times that of the surface as a whole. Wang *et al.*²⁰ have also reported that the passivation across the surface was by no means uniform, observing a 40% variation in PL intensity from different areas. In an attempt to make the passivation treatment more uniform they subsequently used a $(\text{NH}_4)_2\text{S}$ rinse as their final preparation step, however, our experience of surfaces rinsed in this manner is that they are incompatible with STM imaging.

The ambient oxidation of these passivated surfaces as a function of time was investigated by the STM under two sets of conditions. First, the passivated surface was scanned once a day over a period of eight days to monitor changes in surface profile, and second, a $3 \times 3 \mu\text{m}^2$ area was

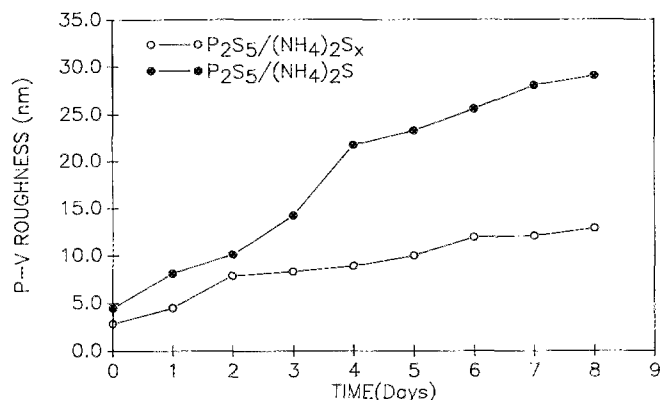


FIG. 2. Surface roughness (PV) plotted as a function of time (in days) for both the $P_2S_5/(NH_4)_2S_x$ (open circles) and the $P_2S_5/(NH_4)_2S$ (closed circles) treated surfaces using a single STM scan to monitor oxide growth.

scanned continuously to monitor the local oxide growth within the scanned area. The reason for imaging the passivated surfaces by these two ways was because we observed that constant STM imaging of the passivated surface causes a rapid increase in the local rate of oxidation. Therefore in order to study the rate of native oxide growth, the exposure of the passivated surface to repeated scanning was minimized. Graphs plotting the change in surface roughness for both passivating solutions over an eight day period are shown in Fig. 2. These results should be compared with the fact that surface roughness values of 40–50 nm (PV) were routinely obtained for the unpassivated surface 1 h after etching. Both surfaces exhibit similar trends, but it is apparent that the $P_2S_5/(NH_4)_2S_x$ treated sample oxidizes at a much slower rate. This becomes increasingly obvious following prolonged exposure to ambient oxidation with the $P_2S_5/(NH_4)_2S_x$ passivated surface displaying surface roughness values one third those of the $P_2S_5/(NH_4)_2S$ treated surface after eight days. These passivating treatments clearly inhibit the native oxide growth to a very significant extent. The difference between the two passivating solutions from our studies is purely quantitative with the $P_2S_5/(NH_4)_2S_x$ solution producing a surface which is more resistive to ambient oxidation. Our results support the proposal made by Nannichi *et al.*¹⁶ that the additional reactive sulfur component in the $P_2S_5/(NH_4)_2S_x$ solution, which etches the GaAs surface, ensures the complete removal of any residual surface oxides following the initial acidic etch.

The changes in surface profile resulting from the oxidation of a passivated surface which was scanned continuously was spatially analyzed. Figures 3(a)–3(f) illustrate the formation and growth of oxide islands on $P_2S_5/(NH_4)_2S_x$ passivated surfaces over a 24 min scanning period. There is a 4 min time lapse present from image to image, this being the time needed to collect STM data for one image at a scan rate of 1.3 Hz. It can be clearly seen that oxide growth is via the formation of nucleation centers dispersed across the semiconductor surface which grow and coalesce. The islands appearing brightest in Fig. 3 are

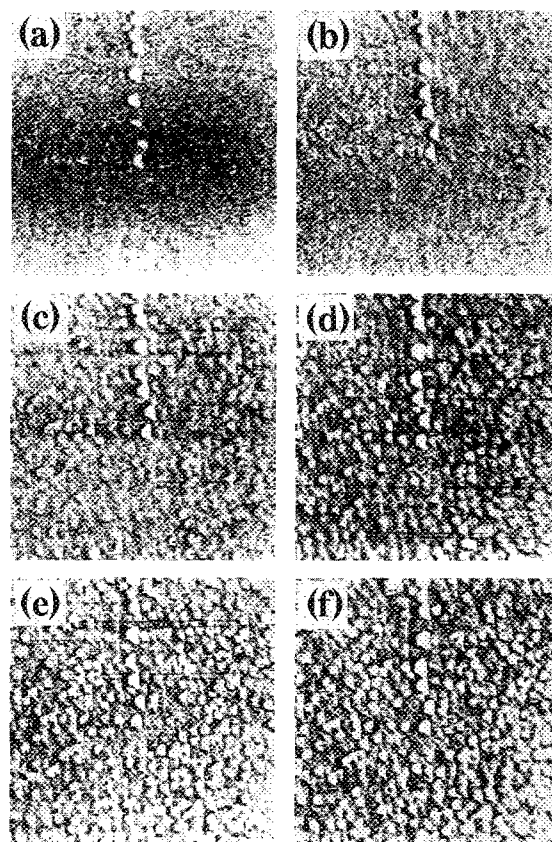


FIG. 3. Oxide growth across a $5 \times 5 \mu m^2$ area of the $P_2S_5/(NH_4)_2S$ treated GaAs(100) surface over a continual scanning period of 24 min. (Scan rate = 1.3 Hz.) Note the formation of oxide islands.

due to tip bias pulsing effects discussed below. It has been suggested in a STM study of imaging multiquantum well structures in air²⁵ that surface oxidation may be accelerated by the tunneling current. In order to investigate this effect on GaAs, a $P_2S_5/(NH_4)_2S$ passivated surface was scanned over a $3 \times 3 \mu m^2$ area continuously for 1 h. By then increasing the scan area to $12 \times 12 \mu m^2$ area, it was possible to note the effects of prolonged scanning on the oxidation process. In Fig. 4, the continuously scanned area on the right is quite dramatically oxidized when compared to the square towards the center (scanned 12 times) and the surrounding surface (scanned twice). The enhanced roughening of the surface is dependent on both the tunneling current and bias voltages. By raising the tunneling current to 5 from 1 nA, thereby reducing the tip-sample distance, and increasing the bias voltage to -4.5 from -3.8 V, areas such as that observed on the right-hand side of Fig. 4 can be created. A more dramatic illustration of this dependence is presented in Fig. 3(a), where a line of oxide islands, ~ 150 nm wide, was created via pulsing the surface a number of times by increasing the tip bias to a value of -7 V for $500 \mu m$ (during an interruption in the feedback loop, i.e., tunneling gap was kept constant). As the surrounding oxide islands form and grow, the fabricated oxide line becomes increasingly indistinguishable from the native oxide. Continuous oxide lines, of ~ 100 nm width, have

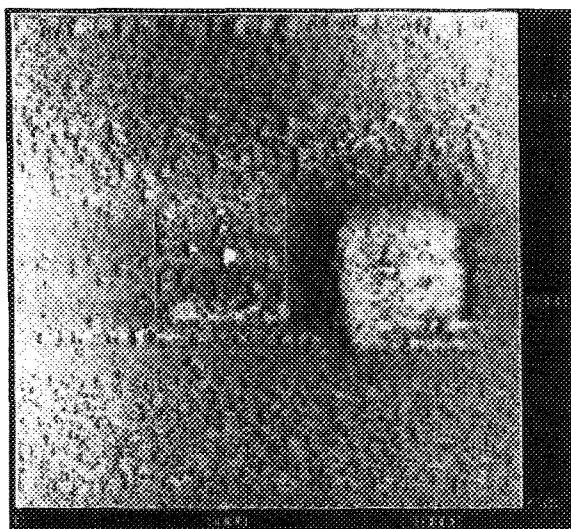


FIG. 4. The effect of continual STM scanning on a $3 \times 3 \mu\text{m}^2$ region of the passivated surface within a $12 \times 12 \mu\text{m}^2$ area. Note how the square area on the right is much more dramatically oxidized in comparison to the center region (scanned 12 times) and the rest of the surface (scanned twice).

been formed by disabling the y -piezo voltage of the tube scanner and increasing bias voltage and tunnel current as described above.

Figure 5 illustrates the change in surface roughness as a function of scanning time up to 1 h. We propose that the initial rapid change in surface roughness results from the STM disrupting the surface passivating layer in the area being scanned and enhancing oxidation of the underlying surface. This is followed by a more gradual increase in surface roughness reflecting the subsequent slower rate of surface oxidation. Previous studies of the ambient oxidation of GaAs have also reported an initial rapid oxidation phase followed by a much slower logarithmic growth rate.²⁶ The fact that little difference in the profile of the roughness curves was observed for the two passivating solutions supports the idea that the STM disrupts the passivating layer. The relative improvement in resistance to am-

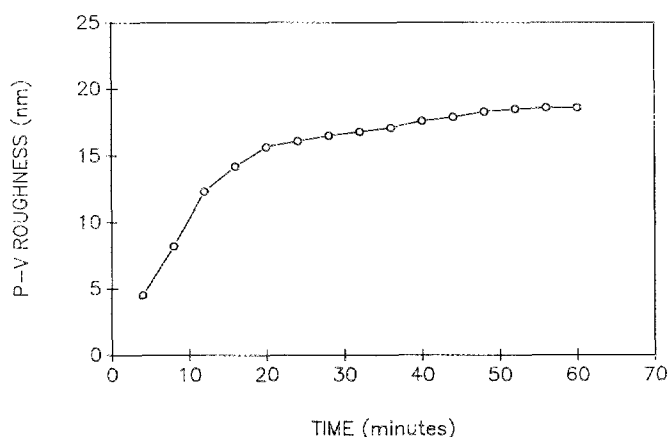


FIG. 5. Surface roughness plotted as a function of scanning time. No significant difference in profile of this curve was noted for the two passivating solutions.

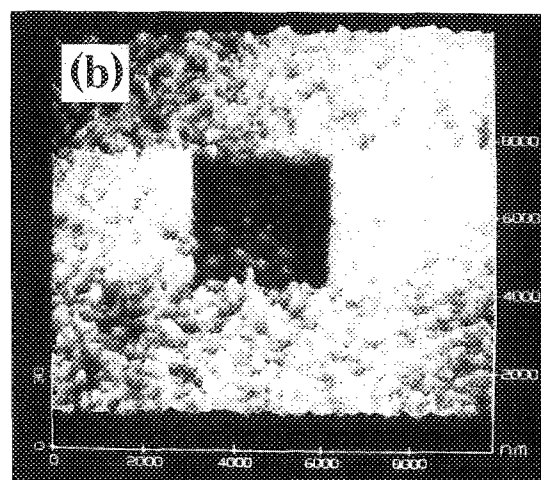
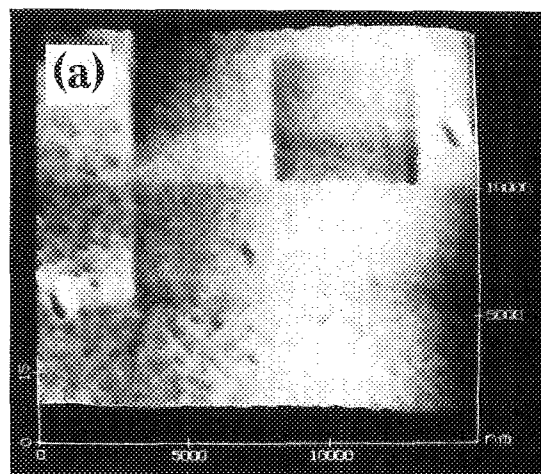


FIG. 6. (a) Grey-scale surface plot and (b) section through scanning squares caused by a field desorption process of the STM. The apparent depth of these squares from (b) is ~ 1 ML. (c) A 5 nm apparent depth square fabricated on a more oxidized $\text{P}_2\text{S}_5/(\text{NH}_4)_2\text{S}_x$ surface.

bient oxidation observed for the $\text{P}_2\text{S}_5/(\text{NH}_4)_2\text{S}_x$ treated surface is therefore lost due to the magnitude of this scanning effect. There is, very noticeably, a significant difference in the general shape of the oxide islands that form on continuously scanned areas as opposed to those scanned only once. This is immediately apparent when the images of Figs. 1 and 2 are compared. While we do not have a satisfactory explanation for this observation, it is possibly that the STM's scanning effect not only causes an increased oxidation rate but also influences the spatial distribution of the products of the oxygen-substrate reaction.

Dagata *et al.*²² have pioneered STM-based pattern generation and nanolithography on passivated GaAs surfaces. This process involves the modification of the passivated surface directly with the STM. It can result in the formation of "scanning squares" due to the raster scan mechanism of the tunneling microscope. In our studies of the passivated surfaces, we have observed scanning squares with the apparent depth ranging from ~ 1 ML (0.3 nm) to 5 nm. Local conductivity changes contribute to the apparent depth of these features. Figure 6(a) illustrates two such

superimposed squares, each being 0.3 nm in depth, fabricated on a $P_2S_5/(NH_4)_2S_x$ passivated surface after 30 min in air, with Fig. 6(b) illustrating a 5 nm deep square formed on a more oxidized, similarly treated surface. Scanning square creation has been found to be a function of time/scan rate, there is a minimum number of times an area must be scanned at a certain scan rate before a square is created. Surface quality plays an important part in the formation, when the surface is heavily oxidized no square is created no matter how many times the area is scanned. Only when the surface is well passivated and very smooth can these features be created. There is, furthermore, a local increase in rate of oxidation within these squares, even when they are not continuously scanned. This would suggest that the formation mechanism of these features is related to the disruption of the passivated surface by the scanning process. Finally, no LEED patterns were observed on any of the passivated GaAs surfaces detailed in this study, suggesting that no ideal sulfur termination of the GaAs(100) surface results from using these treatments as described.

B. Scanning tunneling spectroscopy (STS) analysis

STS studies of both chemically etched and $P_2S_5/(NH_4)_2S_x$ treated surfaces were also undertaken. In the case of such tunneling spectroscopy, the difference between the work function of the tip and the semiconductor electron affinity results in the formation of a potential barrier at the interface.²⁷ The current-voltage (I - V) characteristics reproduced in Fig. 7(a) represent those of the $P_2S_5/(NH_4)_2S_x$ passivated and an unpassivated GaAs surface. Acquisition of these characteristics was performed (using Nanoscope II software), after it was ensured that the STM images were noise-free and that tip condition was good. The bias voltage (-500 mV), applied in spectroscopic plot mode (feedback loop initially on), establishes a fixed tip-sample separation, whereupon the feedback loop is opened and the bias voltage ramped from -3.0 to $+3.0$ V. Normally, three to five separate I - V data files were averaged to provide an accurate representation of the I - V relationship. From Fig. 7(a) it is immediately apparent, without any further analysis, that there is a narrowing of the region of minimum conductivity (the band gap) when the passivated surface is compared to the unpassivated. As recently shown by Dagata and Tseng,²⁸ this behavior is consistent with the I - V properties of the cleaved GaAs(110) surface oxidized in ultrahigh vacuum (UHV).²⁹ The surface oxidation leads to surface state induced band bending which significantly attenuates the contribution of dopant-induced states in the semiconductor conduction band to the I - V spectrum.^{29,30} The narrow band gap noted on the passivated surface is possibly a result of residual surface defects causing a small degree of band bending. Comparable STS investigations on $P_2S_5/(NH_4)_2S_x$ passivated InP(100) surfaces indicate that this narrow gap is reduced still further.³¹

The quantity $(dI/dV)/(I/V)$ provides a measure of the surface state density which is approximately independent of the tip-sample separation.³² By plotting this quantity

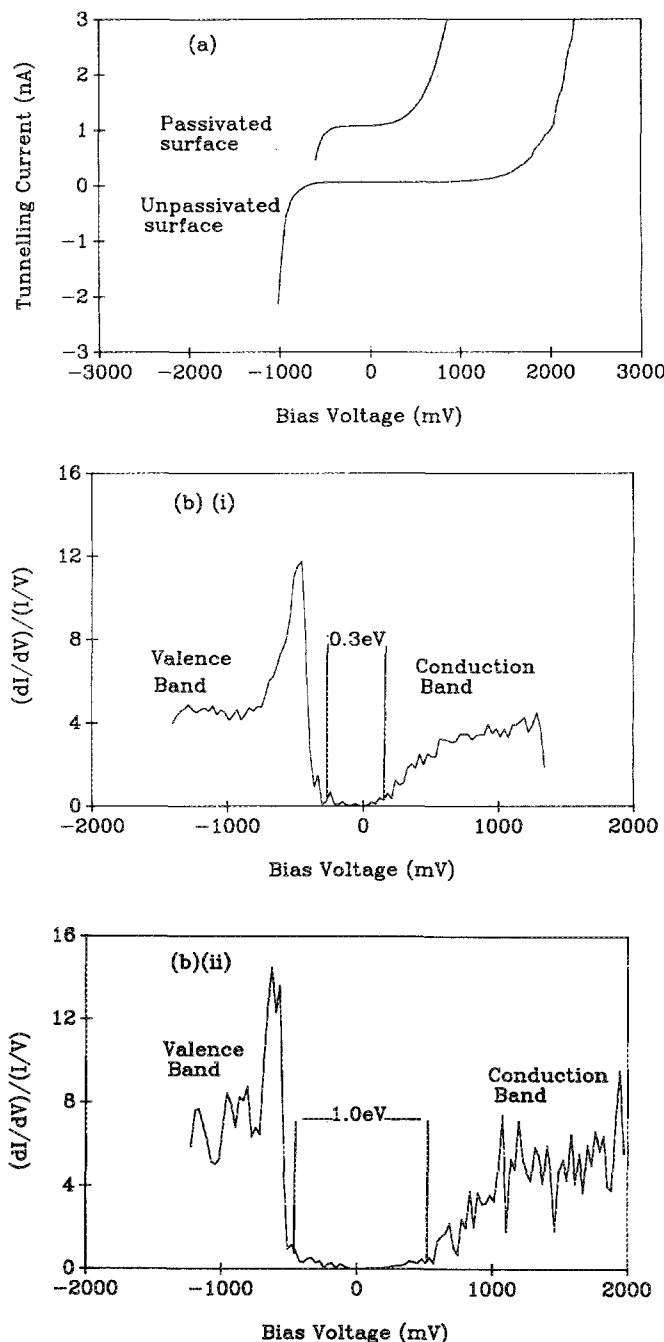


FIG. 7. (a) STM I - V spectroscopy data for both the chemically etched GaAs(100) surface and the $P_2S_5/(NH_4)_2S_x$ passivated surface. (b) Normalized differential conductance vs bias voltage plot for (i) well-passivated region of GaAs(100) surface and (ii) within STM scan induced oxide region. Note widening of "band gap."

versus the bias voltage, a gap of ~ 0.3 eV for the passivated and 1.2 eV for the unpassivated surface was noted. Figures 7(b) and 7(c) represent plots of normalized differential conductivity versus bias voltage at well-passivated and STM scanned surface regions. The 0 V bias voltage level represents the Fermi-level position. Again, it is evident that a wider band gap is measured on the roughened region (~ 1.0 eV), supporting the suggestion that this roughening is due to a STM scan induced surface oxide. Furthermore, the Fermi-level position has moved from close to the con-

duction band edge in Fig. 7(b) to approximately midgap in Fig. 7(c), which mirrors the Fermi-level position for the unpassivated sample.

IV. CONCLUSIONS

The ambient oxidation of GaAs(100) surfaces treated with P_2S_5 containing $(NH_4)_2S$ and $(NH_4)_2S_x$ solutions has been investigated by STM. Both treatments have been shown to be capable of producing chemically uniform, physically flat surfaces which are resistant to ambient oxidation, with the $P_2S_5/(NH_4)_2S_x$ treated surfaces displaying quantitatively enhanced passivation properties. The presence of phosphorus on the sulfur passivated surfaces appears to play a significant role in determining the initial surface roughness and the resistance of the surface to ambient oxidation. Continual scanning of a region of the passivated surface by the STM results in a substantial increase in the local rate of oxide growth. $I-V$ spectroscopy measurements, with the STM, have shown that the passivating treatment reduces the surface state density to the extent that little band bending in the spectra is noted. The Fermi-level position subsequently moves from close to the conduction band edge to near midgap as a function of surface oxidation.

ACKNOWLEDGMENTS

The authors would like to thank The Metrology Laboratory at EOLAS (The Irish Science and Technology Agency) for providing access to the STM used in these studies. P. M. and B. M. acknowledge funding from the EOLAS Applied Science Award Scheme and the Strategic Research Programme, respectively.

¹E. Yablonovitch, C. J. Sandroff, R. Bhat, and T. Gmitter, *Appl. Phys. Lett.* **51**, 439 (1987).

²R. S. Besser and C. R. Helms, *Appl. Phys. Lett.* **52**, 1707 (1988).

³D. Liu, T. Zhang, R. A. LaRue, J. S. Harris, Jr., and T. W. Sigmon, *Appl. Phys. Lett.* **53**, 1059 (1988).

⁴J. Fan, H. Oigawa, and Y. Nannichi, *Jpn. J. Appl. Phys.* **27**, L2125 (1988).

⁵J. E. Samaras and R. B. Darling, *J. Appl. Phys.* **72**, 168 (1992).

⁶C. O. Thermond, G. P. Schwartz, G. W. Kammlot, and B. Schwartz, *J. Electrochem. Soc.* **127**, 1366 (1980).

⁷E. Capasso and G. F. Williams, *J. Electrochem. Soc.* **129**, 921 (1982).

⁸W. E. Spicer, P. W. Chye, P. R. Skeath, C. Y. Su, and I. Lindau, *J. Vac. Sci. Technol.* **16**, 1422 (1979).

⁹M. S. Carpenter, M. R. Melloch, B. A. Cowans, Z. Dardas, and W. M. Delglass, *J. Vac. Sci. Technol. B* **7**, 845 (1988).

¹⁰R. Richter and H. L. Hartnagel, *J. Electrochem. Soc.* **137**, 2879 (1990).

¹¹J. Shin, K. M. Geib, and C. W. Wilmsen, *J. Vac. Sci. Technol. B* **9**, 2337 (1991).

¹²H. Sugahara, M. Oshima, H. Owigawa, H. Shigekawa, and Y. Nannichi, *Extended Abstracts 21st Conference Solid State Devices and Materials*, Toyoko, 1989 (Business Centre for Academic Societies Japan, Toyoko, 1989), p. 547.

¹³Y. Takakuma, M. Niwano, S. Fujita, Y. Takeda, and N. Miyamoto, *Appl. Phys. Lett.* **58**, 1635 (1991).

¹⁴C. J. Sandroff, M. S. Hegde, L. A. Farrow, C. C. Chang, and J. P. Haribson, *Appl. Phys. Lett.* **54**, 362 (1989).

¹⁵J. Fan, H. Oigawa, and Y. Nannichi, *Jpn. J. Appl. Phys.* **27**, L2125 (1988).

¹⁶Y. Nannichi, J. Fan, H. Oigawa, and A. Koma, *Jpn. J. Appl. Phys.* **27**, L2367 (1988).

¹⁷H. Oigawa, J. Fan, Y. Nannichi, H. Sugahara, and M. Oshima, *Jpn. J. Appl. Phys.* **30**, L322 (1991).

¹⁸O. Kubaschewski and C. B. Alcock, *Metallurgical Thermochemistry*, 5th ed. (Pergamon, New York, 1979).

¹⁹H. H. Lee, R. J. Raciot, and S. H. Lee, *Appl. Phys. Lett.* **54**, 724 (1989).

²⁰Y. Wang, Y. Darici, and P. H. Holloway, *J. Appl. Phys.* **71**, 2746 (1992).

²¹J. A. Dagata, J. Schneir, H. H. Harary, J. Bennett, and W. Tseng, *J. Vac. Sci. Technol. B* **9**, 1384 (1991).

²²J. A. Dagata, W. Tseng, J. Bennett, J. Schneir, and H. H. Harary, *Appl. Phys. Lett.* **59**, 3288 (1991).

²³J. A. Dagata, W. Tseng, J. Bennett, E. A. Dobisz, J. Schneir, and H. H. Harary, *J. Vac. Sci. Technol. A* **10**, 2105 (1992).

²⁴H. Hirayama, Y. Matsumoto, H. Oigawa, and Y. Nannichi, *Appl. Phys. Lett.* **54**, 2565 (1989).

²⁵I. Tanaka, T. Kato, S. Ohkuochi, and F. Osaka, *J. Vac. Sci. Technol. A* **8**, 567 (1990).

²⁶F. Lukes, *Surf. Sci.* **30**, 91 (1972).

²⁷W. J. Kaiser, L. D. Bell, M. H. Hecht, and F. J. Grunthaner, *J. Vac. Sci. Technol. A* **6**, 519 (1988).

²⁸J. A. Dagata and W. Tseng, *Appl. Phys. Lett.* **62**, 591 (1993).

²⁹R. M. Feenstra and J. A. Strosio, *J. Vac. Sci. Technol. B* **5**, 923 (1987).

³⁰J. A. Strosio and R. M. Feenstra, *J. Vac. Sci. Technol. B* **6**, 1472 (1988).

³¹B. Murphy, P. Moriarty, and G. Hughes (unpublished).

³²J. A. Strosio, R. M. Feenstra, and A. P. Fein, *Phys. Rev. Lett.* **61**, 447 (1988).